International Journal of Science and Research (IJSR)
ISSN (Online): 2319-7064
Index Copernicus Value (2013): 6.14 | Impact Factor (2013): 4.438

Consequences of Interphase between Matrix and Reinforced Nanoparticle on Behavior of AA6262/AlN Nanocomposites

A. Chennakesava Reddy

Professor, Department of Mechanical Engineering, JNTUH College of Engineering, Kukatpally, Hyderabad – 500 085, Telangana, India

Abstract: ***The performance of the metal matrix particulate composite depends, besides the matrix microstructure and the nature of the reinforcement, very significantly on the interphase between matrix and reinforcement. Improvements in mechanical properties have been found by adding a wetting agent. In this article two types of RVE models have been executed using finite element analysis. Aluminum nitride nanoparticles were used as a reinforcing material in the matrix of AA6262 aluminum alloy. It has been ob-served that the nanoparticle did not overload during the transfer of load from the matrix to the nanoparticle via the interphase due to interphase between the nanoparticle and the matrix. The tensile strength has increased from 305.61 to 314.70 MPa with interphase around aluminum nitride nanoparticle in the AA6262/AlN nanocomposites.***

Keywords: RVE models, AlN, AA6262, finite element analysis, interphase.

1. Introduction

Metal matrix composites (MMCs) have been drawn attention in recent years resulting from the need for materials with high strength and stiffness in the field for a large number of functional and structural applications. The higher stiffness of ceramic particles can lead to an incremental increase in the stiffness of a composite [1, 2]. One of the major challenges when processing nanocomposites is achieving a homogeneous distribution of reinforcement in the matrix as it has a strong impact on the properties and the quality of the material. The current processing methods often generate agglomerated particles in the ductile matrix and as a result they exhibit extremely low ductility [3]. Particle clusters act as crack or decohesion nucleation sites at stresses lower than the matrix yield strength, causing the nanocomposite to fail at unpredictable low stress levels. Possible reasons resulting in particle clustering are chemical binding, surface energy reduction or particle segregation [4, 5, 6]. While manufacturing Al alloy/AlN nanocomposites, the wettability factor is the major concern irrespective of the manufacturing method. Its superior surface activity restricts its incorporation in the metal matrix. One of the methods is to add surfactant which acts as a wetting agent in molten metal to enhance wettability of particulates. Researchers have successfully used several surfactants like Li, Mg, Ca, Zr, Ti, Cu, and Si for the synthesis of nanocomposites [7, 8, 9].

The objective of this article was to develop AA6262/AlN nanocomposites with and without wetting criteria of AlN by AA6262 molten metal. RVE models were used to analyze the nanocomposites using finite element analysis. A homogeneous interphase region was assumed in the models.

2. Theoretical Background

Analyzing structures on a microstructural level, however, are clearly an inflexible problem. Analysis methods have therefore sought to approximate composite structural mechanics by analyzing a representative section of the composite microstructure, commonly called a Representative Volume Element (RVE). One of the first formal definitions of the RVE was given by Hill [10] who stated that the RVE was 1) structurally entirely typical of the composite material on average and 2) contained a sufficient number of inclusions such that the apparent moduli were independent of the RVE boundary displacements or tractions. Under axisymmetric as well as antisymmetric loading, a 2-D axisymmetric model can be used for the cylindrical RVE, which can significantly reduce the computational work [11].

2.1 Determination Effective Material Properties

To derive the formulae for deriving the equivalent material constants, a homogenized elasticity model of the square representative volume element (RVE) is considered. The dimensions of the three-dimensional RVE are $2a$ x $2a$ x $2a$. The cross-sectional area of the RVE is $2a$ x $2a$. The elasticity model is filled with a single, transversely isotropic material that has five independent material constants (elastic moduli E_y and E_z, Poison's ratios v_{xy}, v_{yz} and shear modulus Gyz). The general strain-stress relations relating the normal stresses and the normal stains are given below:

$$\varepsilon_x = \frac{\zeta_x}{E_x} - \frac{v_{xy}\,\zeta_y}{E_y} - \frac{v_{xz}\,\zeta_z}{E_z} \quad (1)$$

$$\varepsilon_y = -\frac{v_{yx}\,\zeta_x}{E_y} + \frac{\zeta_y}{E_y} - \frac{v_{yz}\,\zeta_z}{E_z} \quad (2)$$

$$\varepsilon_z = -\frac{v_{zx}\,\zeta_x}{E_x} - \frac{v_{zy}\,\zeta_y}{E_y} + \frac{\zeta_z}{E_z} \quad (3)$$

Let assume that $\zeta_{xy} = \zeta_{yx}, \zeta_{yz} = \zeta_{zy}$ and $\zeta_{zx} = \zeta_{xz}$. For plane strain conditions, $\epsilon_z = 0, \epsilon_{yz} = \varepsilon_{zx} = 0$ and $\zeta_{yz} = \zeta_{zx}$. The above equations are rewritten as follows:

$$\varepsilon_x = \frac{\zeta_x}{E_x} - \frac{v_{xy}\,\zeta_y}{E_y} - \frac{v_{yz}\,\zeta_z}{E_z} \quad (4)$$

$$\varepsilon_y = -\frac{v_{xy}\,\zeta_x}{E_y} + \frac{\zeta_y}{E_y} - \frac{v_{yz}\,\zeta_z}{E_z} \quad (5)$$

$$\varepsilon_z = -\frac{v_{yz}\,\zeta_x}{E_z} - \frac{v_{yz}\,\zeta_y}{E_z} + \frac{\zeta_z}{E_z} \quad (6)$$

To determine E_y and E_z, v_{xy} and v_{yz}, four equations are required. Two loading cases as illustrated in figure 1 have been designed to give four such equations based on the theory of elasticity. For load case (figure 1a), the stress and strain components on the lateral surface are:

$\zeta_x = \zeta_y = 0$

$\varepsilon_x = \frac{\Delta a}{a}$ along $x = \pm a$ and $\varepsilon_y = \frac{\Delta a}{a}$ along $y = \pm a$

$\varepsilon_z = \frac{\Delta a}{a}$

where Δa is the change of dimension a of cross-section under the stretch Δa in the z-direction. Integrating and averaging Eq. (6) on the plane z = a, the following equation can be arrived:

$$E_z = \frac{\zeta_{ave}}{\varepsilon_z} = \frac{a}{\Delta a}\zeta_{ave} \quad (7)$$

where the average value of ζz is given by:

$$\zeta_{ave} = \iint \zeta_z\,(x, y, a)dxdy \quad (8)$$

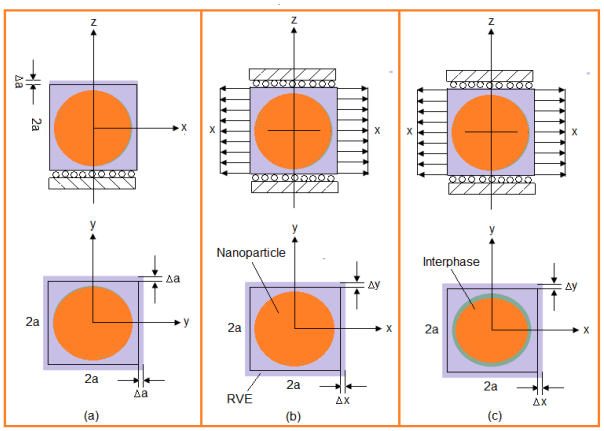

Figure 1: RVE models

The value of ζave is evaluated for the RVE using finite element analysis (FEA) results.

Using Eq. (5) and the result (7), the strain along $y = \pm a$:

$\varepsilon_y = -\frac{\nu_{yz}\zeta_z}{E_z} = -\nu_{yz}\frac{\Delta a}{a} = \frac{\Delta a}{a}$

Hence, the expression for the Poisson's ratio ν_{yz} is as follows:

$$\nu_{yz} = -1 \quad (9)$$

For load case (figure 1b), the square representative volume element (RVE) is loaded with a uniformly distributed load (negative pressure), P in a lateral direction, for instance, the x-direction. The RVE is constrained in the z-direction so that the plane strain condition is sustained to simulate the interactions of RVE with surrounding materials in the z-direction. Since $\varepsilon_z = 0$, $\zeta_z = \nu_{yz}(\zeta_x + \zeta_y)$ for the plain stress, the strain-stress relations can be reduced as follows:

$$\varepsilon_x = \left(\frac{1}{E_x} - \frac{1}{E_z}\right)\zeta_x - \left(\frac{\nu_{xy}}{E_y} + \frac{1}{E_z}\right)\zeta_y \quad (10)$$

$$\varepsilon_y = -\left(\frac{\nu_{xy}}{E_x} + \frac{1}{E_z}\right)\zeta_x + \left(\frac{1}{E_x} - \frac{1}{E_z}\right)\zeta_y \quad (11)$$

For the elasticity model as shown in figure 1b, one can have the following results for the normal stress and strain components at a point on the lateral surface:

$\zeta_y = 0, \zeta_x = P$

$\varepsilon_x = \frac{\Delta x}{a}$ along $x = \pm a$ and $\varepsilon_y = \frac{\Delta y}{a}$ along $y = \pm a$

where Δx (>0) and Δy (<0) are the changes of dimensions in the x- and y- direction, respectively for the load case shown in figure 2b. Applying Eq. (11) for points along $y = \pm a$ and Eq. (10) for points along $x = \pm a$, we get the following:

$$\varepsilon_y = -\left(\frac{\nu_{xy}}{E_x} + \frac{1}{E_z}\right)P = \frac{\Delta y}{a} \quad (12)$$

$$\varepsilon_x = \left(\frac{1}{E_x} - \frac{1}{E_z}\right)P = \frac{\Delta x}{a} \quad (13)$$

By solving Eqs. (12) and (13), the effective elastic modulus and Poisson's ratio in the transverse direction (xy-plane) as follows:

$$E_x = E_y = \frac{1}{\frac{\Delta x}{Pa} + \frac{1}{E_z}} \quad (14)$$

$$\nu_{xy} = \left(\frac{\Delta y}{Pa} + \frac{1}{E_z}\right)\Big/\left(\frac{\Delta x}{Pa} + \frac{1}{E_z}\right) \quad (15)$$

In which Ez can be determined from Eq. (7). Once the change in lengths along x- and y- direction (Δx and Δy) are determined for the square RVE from the FEA, E_y (= E_x) and vxy can be determined from Eqs. (14) and (15), correspondingly.

2.2 Empirical models for elastic moduli and strength

The strength of a particulate metal matrix composite depends on the strength of the weakest zone and metallurgical phenomena in it [12, 13]. A new criterion is suggested by the author considering adhesion, formation of precipitates, particle size, agglomeration, voids/porosity, obstacles to the dislocation, and the interfacial reaction of the particle/matrix. The formula for the strength of composite is stated below:

$$\zeta_c = \left[\zeta_m\left\{\frac{1-(v_p+v_v)^{2/3}}{1-1.5(v_p+v_v)}\right\}\right]e^{m_p(v_p+v_v)} + kd_p^{-1/2} \quad (16)$$

$$k = E_m m_m / E_p m_p$$

where, v_v and v_p are the volume fractions of voids/porosity and nanoparticles in the composite respectively, m_p and m_m are the possion's ratios of the nanoparticles and matrix respectively, d_p is the mean nanoparticle size (diameter) and E_m and E_p are elastic moduli of the matrix and the particle respectively. Elastic modulus (Young's modulus) is a measure of the stiffness of a material and is a quantity used to characterize materials. Elastic modulus is same in all orientations for isotropic materials. Anisotropy can be seen in many composites. The proposed equations [12, 13] by the author to find Young's modulus of composites and interphase including the effect of voids/porosity as given below:

The upper-bound equation is given by

$$\frac{E_c}{E_m} = \left(\frac{1-v_v^{2/3}}{1-v_v^{2/3}+v_v}\right) + \frac{1+(\delta-1)v_p^{2/3}}{1+(\delta-1)(v_p^{2/3}-v_p)} \quad (17)$$

The lower-bound equation is given by

$$\frac{E_c}{E_m} = 1 + \frac{v_p - v_p}{\delta/(\delta-1)-(v_p+v_v)^{1/3}} \quad (18)$$

where, $\delta = E_p/E_m$.

The transverse modulus is given by

$$E_t = \frac{E_m E_p}{E_m + E_p(1-v_p^{2/3})/v_p^{2/3}} + E_m\left(1 - v_p^{2/3} - v_v^{2/3}\right) \quad (19)$$

The young's modulus of the interphase is obtained by the following formula:

$$E_i(r) = (\alpha E_p - E_m)\left(\frac{r_i - r}{r_i - r_p}\right) + E_m \quad (20)$$

3. Materials Methods

The matrix material was AA6262 aluminum alloy. AA6262 contains Si (12.50%), Cr (≤0.10%), Cu (1.20%), Fe (≤1.00%), Mg (1.10%), Ni (1.00%) and Zn (≤0.25%) as its major alloying elements. The reinforcement material was aluminum nitride (AlN) nanoparticles of average size 100nm. The mechanical properties of materials used in the present work are given in table 1.

Table 1: Mechanical properties of AA6262 matrix and AlN nanoparticles

Property	AA6262	AlN
Density, g/cc	2.72	3.26
Elastic modulus, GPa	69.0	330
Ultimate tensile strength, MPa	220	270
Poisson's ratio	0.33	0.24

The representative volume element (RVE or the unit cell) is the smallest volume over which a measurement can be made that will yield a value representative of the whole. In this research, a cubical RVE was implemented to analyze the tensile behavior AA6262/AlN nanocomposites (figure 6). The determination of the RVE's dimensional conditions requires the establishment of a volumetric fraction of spherical nanoparticles in the composite. Hence, the weight fractions of the particles were converted to volume fractions. The volume fraction of a particle in the RVE ($V_{p,rve}$) is determined using Eq.(21):

$$v_{p,rve} = \frac{Volume\ \ of\ nanoparticle}{Volume\ \ of\ RVE} = \frac{16}{3} \times \left(\frac{r}{a}\right)^3 \quad (21)$$

where, r represents the particle radius and a indicates the diameter of the cylindrical RVE. The volume fraction of the particles in the composite (V_p) is obtained using equation

$$V_p = (w_p/\rho_p)/(w_p/\rho_p + w_m/\rho_m) \quad (22)$$

where ρ_m and ρ_p denote the matrix and particle densities, and w_m and w_p indicate the matrix and particle weight fractions, respectively.

The RVE dimension (a) was determined by equalizing Eqs. (21) and (22). Two RVE schemes namely: without interphase (adhesion) and with interphase were applied between the matrix and the filler. The loading on the RVE was defined as symmetric displacement, which provided equal displacements at both ends of the RVE. To obtain the nanocomposite modulus and yield strength, the force reaction was defined against displacement. The large strain PLANE183 element [14] was used in the matrix and the interphase regions in all the models. In order to model the adhesion between the interphase and the particle, a COMBIN14 spring-damper element was used. The stiffness of this element was taken as unity for perfect adhesion which could determine the interfacial strength for the interface region. To achieve convergence of an exact nonlinear solution, it was important to set the strain rates of the FEM models based on the experimental tensile tests' setups. Hence, FEM models of different RVEs with various particle contents should have comparable error values. In this respect, the ratio of the tensile test speed to the gauge length of the specimens should be equal to the corresponding ratio in the RVE displacement model. Therefore, the rate of displacement in the RVEs was set to be 0.1 (1/min).

4. Results and Discussion

The AlN/AA6262 nanocomposites with or without interphase were modeled using finite element analysis (ANSYS) to analyze the tensile behavior and fracture.

4.1 Tensile behavior

An increase of AlN content in the matrix could increase the tensile strength of the nanocomposite (figure 2). The maximum difference between the results by FEA without interphase and those of experimentation was 48.53 MPa. This differentiation can be attributed to lack of bonding between the AlN nanoparticle and the AA6262 matrix. The maximum difference between the results obtained by FEA with interphase and those of experimentation was 54.12 MPa. This discrepancy can be endorsed to the presence of voids in the nanocomposites. The results obtained from author's model (with voids) were almost equal to those of experimentation with difference of 5.21 MPa.

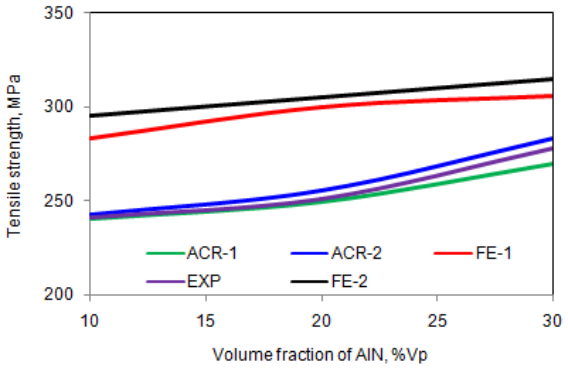

Figure 2: Effect of volume fraction on tensile strength along tensile load direction.

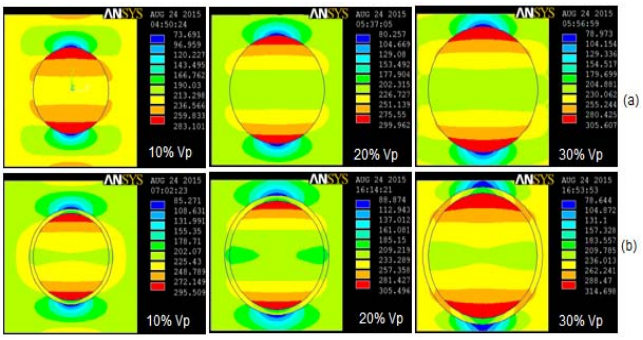

Figure 3: Tensile stresses (a) without interphase and (b) with interphase normal to load direction.

For 10%, 20% and 30%Vp of AlN in AA6262, without interphase and barely consideration of adhesive bonding between the AlN nanoparticle and the AA6262 matrix, the loads transferred from the AlN nanoparticle to the AA6262 matrix were, respectively, 46.54 MPa, 73.24 MPa and 75.55 MPa (figure 3) along the tensile load direction. Similarly, for 10%, 20% and 30%Vp of AlN in AA6262, with interphase and wet-ting between the ALN nanoparticle and the AA6262 matrix, the loads transferred from the AlN nanoparticle to the AA6262 matrix were, respectively,70.08 MPa, 96.28 MPa and 78.69 MPa (figure 3) along the tensile load direction. Zhengang et al [15] carried a study improving wettability by adding Mg as the wetting agent. They found that the wettability between molten Al-Mg matrix and SiC particles is improved and the surface tension of molten Al-Mg alloy with SiC particle is reduced, and results in homogeneous particles distribution and high interfacial bond strength. For instance, addition of Mg to composite matrix lead to the formation of MgO and $MgAl_2O_3$ at the interface and this increases the wettability and the strength of the composite [16]. The longitudinal elastic moduli increased appreciably (table 2) with interphase around AlN nanoparticles. The longitudinal and transverse moduli increased with increase of AlN content up to 20% Vp and later they decreased.

Table 2: Elastic moduli of AA6262/AlN nano composite

Source	Criteria	E_{cl}/E_m			E_{ct}/E_m		
		Vp = 10%	Vp = 20%	Vp = 30%	Vp = 10%	Vp = 20%	Vp = 30%
FEA	without interphase	1.22	1.27	1.24	1.23	1.27	1.24
FEA	with inter-phase	1.27	1.33	1.26	1.29	1.33	1.26
Author	upper limit	1.24	2.58	2.81	1.02	1.08	1.19
Author	lower limit	1.12	1.20	1.29	-	-	-
Rule of Mixture		1.43	1.80	2.18	1.15	1.25	1.38

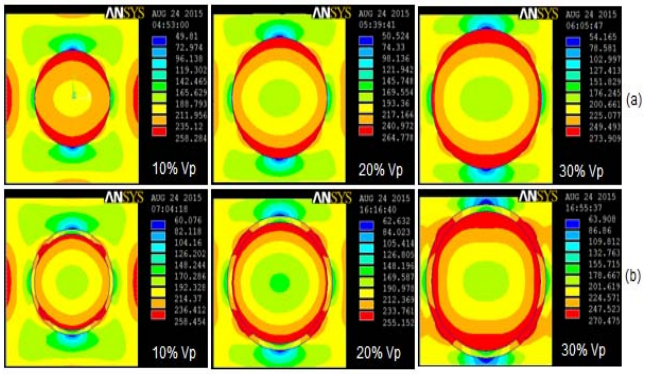

Figure 4: von Mises stress (a) and shear stress (b).

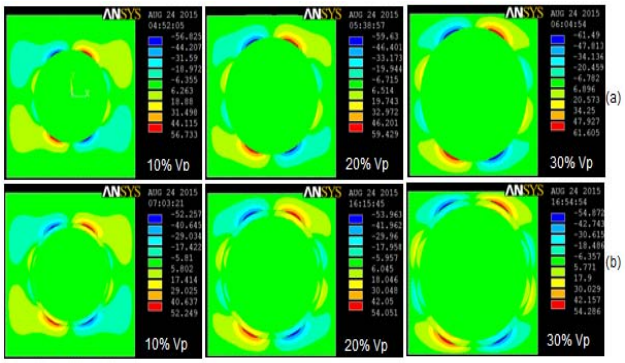

Figure 5: Shear Stresses

4.2 Fracture

Figure 4 depicts the increase of von Mises stress with increase of volume fraction of AlN. The shear stresses induced in the nanocomposites with and without interphase are shown in figure 5. In the case of nanocomposites with interphase between the nanoparticle and the matrix, the stress was transferred through shear from the matrix to the particles resulting low stress in the matrix. The stress transfer from the matrix to the nanoparticle was less for the nanocomposites without interphase resulting high stress in the matrix. Landis and McMeeking [17] assumed that the fibers carry the entire axial load, and the matrix material only transmits shear between the fibers. Based on these assumptions alone, it is widely accepted that these methods are accurate when the fiber volume fraction v_f and the fiber-to matrix moduli ratio E_f/E_m are high. In the present case the elastic moduli of AlN nanoparticle and AA6262 matrix are, respectively, 330 GPa and 69.0 GPa.

5. Conclusion

RVE models give the trend of phenomenon happening in the nanocomposites. Without interphase and bare consideration of adhesive bonding, the tensile strength has been found to be 305.61 MPa for the nanocomposites consisting of 30%Aln nanoparticles. Due to interphase between the nanoparticle and the matrix, the tensile strength increases to 314.70 MPa. The tensile strengths obtained by author's model (with voids) agree well with the experimental results. In the case of nanocomposites with interphase between the nanoparticle and the matrix, the stress is transferred through shear from the matrix to the particles. The transverse moduli of AlN/AA6262 nanocomposites have been found to be 84.56 GPa and 87.56 GPa, respectively, without and with interphase.

Acknowledgements

The author thanks the University Grants Commission (UGC), New Delhi for sanctioning this major project. The author also thanks the Central University, Hyderabad for providing the SEM images to complete this manuscript.

References

[1] A.Chennakesava Reddy, "Mechanical properties and fracture behavior of 6061/SiCp Metal Matrix Composites Fabricated by Low Pressure Die Casting Process," Journal of Manufacturing Technology Research, vol.1, no.3/4, pp. 273-286, 2009.

[2] A.Chennakesava Reddy and Essa Zitoun, "Tensile properties and fracture behavior of 6061/Al_2O_3 metal matrix composites fabricated by low pressure die casting process," International Journal of Materials Sciences, vol. 6, no.2, pp. 147-157, 2011.

[3] X. Deng and N. Chawla, "Modeling the effect of particle clustering on the mechanical behavior of SiC particle reinforced Al matrix composites," Journal of Materials Science, vol.41, pp.5731–5734, 2006.

[4] A.J. Reeves, H. Dunlop and T.W. Clyne, "The effect of interfacial reaction layer thickness on fracture of titanium–SiC particulate composites," Metallurgical Transactions A, vol.23, pp.977–988, 1992.

[5] B. Kotiveerachari, A, Chennakesava Reddy, "Interfacial effect on the fracture mechanism in GFRP composites," CEMILAC Conference, Ministry of Defense, India, 1999, vol.1(b), pp.85-87.

[6] A. Chennakesava Reddy, "Analysis of the Relationship Between the Interface Structure and the Strength of Carbon-Aluminum Composites," NATCON-ME, Bangalore, 13-14th March, 2004, pp.61-62.

[7] S. Ren, X. Shen, X. Qu and X. He, "Effect of Mg and Si on infiltration behavior of Al alloys pressureless infiltration into porous SiCp preforms," International Journal Minerals, Metallurgy and Materials, vol.18, no.6, pp.703–708, 2011.

[8] N. Sobczak, M. Ksiazek, W. Radziwill, J. Morgiel, W. Baliga and L. Stobierski, "Effect of titanium on wettability and interfaces in the Al/ SiC system," in: Proceed-

ings of the International Conference High Temperature Capillarity, Cracow, Poland, 29 June–2 July 1997.
[9] A.M. Davidson and D. Regener, "A comparison of aluminium based metal matrix composites reinforced with coated and uncoated particulate silicon carbide," Composites Science and Technology, vol. 60, no.6, pp.865-869, 2000.
[10] R. Hill, "Elastic properties of reinforced solids: some theoretical principles," Journal of the Mechanics and Physics of Solids, vol.11, pp.357-372, 1963.
[11] Y.J. Liu and X.L. Chen, "Evaluations of the effective material properties of carbon nanotube-based composites using a nanoscale representative volume element", Mechanics of Materials, vol.35, pp.69–81, 2003.
[12] A. Chennakesava Reddy, "Cause and Catastrophe of Strengthening Mechanisms in 6061/Al2O3 Composites Prepared by Stir Casting Process and Validation Using FEA," International Journal of Science and Research, vol. 4, no.2, pp.1272-1281, 2015.
[13] A. Chennakesava Reddy, "Influence of Particle Size, Precipitates, Particle Cracking, Porosity and Clustering of Particles on Tensile Strength of 6061/SiCp Metal Matrix Composites and Validation Using FEA," International Journal of Material Sciences and Manufacturing Engineering," vol.42, no.1, pp.1176-1186, 2015.
[14] Chennakesava R Alavala, "Finite element methods: Basic concepts and applications," PHI Learning Pvt. Ltd, New Delhi, 2008.
[15] Zhengang Liuy, Guoyin Zu, Hongjie Luo, Yihan Liu and Guangchun Yao, "Influence of Mg Addition on Graphite Particle Distribution in the Al Matrix Composites," Journal of Materials Science & Technology, vol.26, no.3, pp.244-pp.244-250, 2010.
[16] A. Chennakesava Reddy and Essa Zitoun, "Matrix alloys for alumina particle reinforced metal matrix composites," Indian Foundry Journal, vol. 55, no.1, pp.12-16, 2009.
[17] C.M. Landis and R.M. McMeeking, "Stress concentrations in composites with interface sliding, matrix stiffness, and uneven fiber spacing using shear lag theory," International Journal of Solids Structures, vol.41, pp. 6289-6313, 1999.